JOURNAL OF CATALYSIS 59, 325–339 (1979)

Hydrocarbon Reactions on Supported Iridium Catalysts

K. FOGER AND J. R. ANDERSON

CSIRO Division of Materials Science, Catalysis and Surface Science Laboratory, University of Melbourne, Parkville 3052, Victoria, Australia

Received November 29, 1978; revised March 7, 1979

The reactions of ethane, *n*-butane, isobutane, neopentane, neohexane, 2,3-dimethylbutane, and methylcyclopentane have been studied over a range of dispersed iridium catalysts in which the iridium was supported on γ-alumina or Aerosil silica, and $\bar{d}_{Ir}$ lay in the range $\leqslant 1$ to 20 nm. The catalysts were characterized by electron microscopy, hydrogen adsorption, and temperature-programmed desorption of hydrogen. Hydrocarbon hydrogenolysis was the sole reaction pathway, except in the reaction of neopentane over catalysts with $\bar{d}_{Ir}$ of 7 and 20 nm, where some isomerization to isopentane was observed, and in the case of isobutane, where there was some inferential evidence for isomerization to *n*-butane prior to hydrogenolysis. The hydrocarbons fell into one of two classes depending upon the activation energy and the type of hydrogenolysis reaction occurring. Reaction in a C_2-unit mode (ethane the archetypal hydrocarbon) occurred with an activation energy in the region of 175 kJ mol^{-1}, and was the reaction mode for C_I–C_I, C_I–C_{II}, and C_{II}–C_{II} bond types. Reaction in an iso-unit mode (neopentane the archetypal hydrocarbon) occurred with an activation energy in the region of 235 kJ mol^{-1}, and was the reaction mode for C_I–C_{IV}, C_I–C_{III}, and C_{II}–C_{III} bond types. (C_I indicates a primary carbon, etc.) The activation energy and the frequency factor (expressed as rate per surface iridium atom) for reaction in the C_2-unit or the iso-unit mode was independent of $\bar{d}_{Ir}$. Provided the hydrogen pressure was kept sufficiently high, all reaction rates were proportional to $P^{1}_{HC}\,P^{-3}_{H_2}$. The reaction mechanism is discussed and is compared with the behavior of the corresponding reactions over platinum catalysts.

The need for efficient reforming catalysts to improve the octane number in gasoline has initiated research into various new catalyst systems, especially since in many countries restrictions have been imposed on lead additives. Instead of platinum alone, alloys of platinum with other transition metals have been investigated as reforming catalysts, and one of the most promising of these seems to be the platinum–iridium system (*1*). Catalysts based on this system have been claimed to show improved activity and selectivity for the formation of desired products, and to have high resistance to coke formation.

So far, little has been published in the open scientific literature concerning the chemistry of catalytic reforming over platinum–iridium catalysts: One of the few publications is from Rasser (*2*).

We take the view that the catalytic chemistry of platinum–iridium is unlikely to be properly understood unless we understand the corresponding catalytic chemistry of platinum and of iridium individually. Whereas the behavior of platinum as a catalyst for the skeletal reactions of hydrocarbons has been studied in some detail (e.g., (*3*)), there is relatively little known about hydrocarbon reactions on iridium.

Clarke and co-workers (*4*, *5*) have ex-

0021-9517/79/120325-15$02.00/0

amined the reaction of butanes on evaporated iridium films. Using supported iridium catalysts, Sinfelt (*6*) studied the hydrogenolysis of ethane in comparison with other group VIII transition metals, and Boudart (*7*) the reaction of neopentane. All groups agree on the high activity of iridium for hydrogenolysis reactions, but whether iridium is able to isomerize molecules like neopentane or isobutane is still an open question. Although Boudart (*7*) reported to have found isomerization of neopentane on iridium supported on silica, Anderson and Avery (*8*) and Clarke *et al.* (*4*, *5*) working with iridium films could not detect any activity for this process.

In the present work we have investigated the reactions of simple hydrocarbons (ethane, *n*-butane, isobutane, neopentane, and neohexane) on iridium catalysts of various dispersions, supported on silica or γ-alumina, characterized by electron microscopy, hydrogen adsorption, and temperature-programmed desorption (TPD) of hydrogen.

EXPERIMENTAL

The reactions were carried out in a single-pass fixed bed reactor operating in a differential mode at low conversions (<10%). The ratio reactor diameter/catalyst particle diameter was >100. The weight of the catalyst used was between 0.2 and 0.5 g. Flow rates of the gas mixtures could be adjusted between 0.2 and 2 $cm^3\ s^{-1}$, with space velocities in the range 1 to 20 s^{-1}. Prior to reaction, the catalyst was reduced in a stream of hydrogen overnight at 620 K; subsequently the catalyst was cooled in a stream of hydrogen to reaction temperature (in the region 410–550 K), and the reactant mixture (normally hydrogen/hydrocarbon, molar ratio, 20/1) was passed over the catalyst at a total pressure of 101 kPa.

Reaction orders in hydrogen and hydrocarbon were obtained by changing the hydrocarbon-to-hydrogen ratio while keeping the total pressure constant, or by diluting the hydrogen stream with inert gas at constant hydrocarbon pressure. The products were analyzed by gas chromatography using a 65-m stainless-steel capillary column coated with HHK (Perkin–Elmer), or a packed column (dimethylsulfolane on firebrick), and a flame ionization detector. The metal content of the catalysts was determined by XRF by comparison with appropriate standards. Further characterization by electron microscopy, hydrogen adsorption, and temperature-programmed desorption used methods previously described (*10*, *11*).

No catalyst deactivation or aging effects were observed provided the reaction system was rigorously protected from traces of adventitious oxygen or water impurity.

Catalysts

Catalysts A. This group of supported iridium catalysts was prepared by impregnation of the support material (Aerosil, Degussa 200; γ-alumina, Harshaw 1401P; both 200 $m^2\ g^{-1}$) with $Ir_4(CO)_{12}$ from a cyclohexane solution. Subsequently the carbonyl was decomposed by heating *in vacuo* or in a flow of nitrogen at 620 to 670 K, and then reduced in hydrogen at those temperatures for at least 15 hr. Details of the preparation have been reported previously (*9*). In addition, a catalyst of large iridium particle size was prepared from a standard catalyst (0.90 wt% Ir/SiO_2) by sintering in hydrogen at 970 K for 3 hr.

Catalysts. B. These catalysts were prepared by impregnation of the support with aqueous chloriridic acid using the method of incipient wetness; the solvent was removed by slow evaporation under vigorous stirring, and the residue was dried at 380 K for several hours and subsequently reduced in a stream of hydrogen at 620 K overnight. In addition, a catalyst of large iridium particle size was prepared by

TABLE 1

Catalyst Characterization

Catalyst[a]	Catalyst origin	$\bar{d}_{Ir}$, mean iridium particle size by electron microscopy (nm)	Saturated H_2 adsorption [molecules H_2 (g Ir)$^{-1}$]	$n_{(s)Ir}$[b]	$N_{(s)Ir}$[c]	D[d]
A_1, 0.90 wt% Ir/SiO_2	$Ir_4(CO)_{12}$	$\leqslant 1.0$	1.58×10^{21}	2.84×10^{19}	3.16×10^{21}	1.0
A_2, 2.50 wt% Ir/γ-Al_2O_3	$Ir_4(CO)_{12}$	$\leqslant 1.0$	—	—	—	~ 1.0[e]
A_3, 0.90 wt% Ir/SiO_2 sintered[f]	$Ir_4(CO)_{12}$	20.0 ± 2	0.089×10^{21}	0.16×10^{19}	0.178×10^{21}	0.057
B_1, 2.40 wt% Ir/γ-Al_2O_3	H_2IrCl_6	1.5 ± 0.2	1.18×10^{21}	5.64×10^{19}	2.36×10^{21}	0.75
B_2, 1.50 wt% Ir/SiO_2	H_2IrCl_6	1.5 ± 0.2	1.20×10^{21}	3.60×10^{19}	2.40×10^{21}	0.77
B_3, 0.98 wt% Ir/SiO_2 calcined[g]	H_2IrCl_6	7.0 ± 1	0.245×10^{21}	0.48×10^{19}	0.490×10^{21}	0.16

[a] Standard preparation unless otherwise specified.
[b] Number of surface iridium atoms per gram of catalyst.
[c] Number of surface iridium atoms per gram of iridium.
[d] Iridium dispersion ($\equiv N_{(s)Ir}/N_{(T)Ir}$): $N_{(T)Ir} = 3.13 \times 10^{21}$ Ir g^{-1}.
[e] Estimated from electron microscopic value of $\bar{d}_{Ir}$.
[f] Sintered, 970 K in hydrogen, 3 h.
[g] Calcined before reduction, 720 K in air, 2 h.

calcining a 0.98-wt% Ir/SiO_2 catalyst in air at 720 K for 2 hr: this was done after impregnation but before hydrogen reduction. After calcination, the sample was hydrogen reduced according to the standard method.

Table 1 summarizes all the catalysts used, including data for characterization by hydrogen adsorption and electron microscopy. Monolayer hydrogen coverage was obtained from the linear portion of the room temperature isotherm, and specific metal surface areas and particle sizes were calculated assuming a stoichiometry of one adsorbed hydrogen atom per surface iridium atom, and assuming spherical particles.

Evaluation

Product distributions are recorded in mole percentages of total products. To avoid, as far as possible, contributions from secondary reaction products, distributions were measured at low conversions (<10%), and initial distributions were obtained by extrapolation to infinite space velocity from a plot of product composition versus reciprocal of space velocity.

Reaction rates were evaluated as turnover numbers (N), molecules per second per surface iridium atom,

$$N = \frac{2.51 \times 10^{17} \times P \times f \times \chi_{HC}}{W_c \times n_{(s)Ir}}, \quad (1)$$

TABLE 2

Reaction Rate Data[a]

Hydrocarbon	Catalyst	Reaction temperature range (K)	Activation energy (kJ mol^{-1})	log (frequency factor) [frequency factor/ molecules s^{-1} $Ir^{-1}_{(s)}$]
Ethane	B_1	503–578	174	14.3
	B_2	503–541	168	13.8
	B_3	522–548	175	15.0
n-Butane	A_1	443–485	173	17.6
	B_1	443–485	174	17.4
	B_2	433–493	170	17.2
	B_3	452–495	172	17.6
Neohexane	A_1	443–485	175	17.2
	B_1	450–495	180	17.9
	B_2	443–485	174	17.1
	B_3	452–495	168	16.0
Isobutane	A_1	493–526	240	21.9
	B_1	498–533	243	22.1
	B_2	493–523	230	21.1
	B_3	509–535	225	20.4
Neopentane	A_1	493–523	246	22.5
	B_1	503–533	251	22.7
	B_2	493–573	239	21.9
	B_3	507–593	230	20.9

[a] Probable errors: activation energy, ±5 kJ mol^{-1}; log (frequency factor), ±1.

where

f reactant flow rate ($cm^3\ s^{-1}$) at 293 K,
χ_{HC} mole fraction of hydrocarbon in feed (usually 0.05),
P percentage conversion,
W_c weight of catalyst (g),
$n_{(s)Ir}$ number of surface iridium atoms per gram of catalyst (from hydrogen adsorption measurements).

RESULTS

Activation Energies and Frequency Factors

Table 2 lists reaction conditions, activation energies, and frequency factors for the reactions of ethane, *n*-butane, neohexane, isobutane, and neopentane on a series of supported iridium catalysts of different dispersions. Arrhenius plots for these reactions are shown in Figs. 1 and 2.

In addition to these data, the reaction of methylcyclopentane was studied over catalyst B_2 ($\bar{d}_{Ir} = 1.5$ nm) in the temperature range 419 to 453 K. Although studied in less detail than the other hydrocarbons, it was nevertheless established that this reaction had an activation energy of about 170 kJ mol^{-1}.

Reaction Orders

Partial pressures of hydrogen and hydrocarbon were changed to measure the orders of the reaction (n, m) with respect to both reactants, according to

$$\text{rate} \propto P^n_{HC} P^m_{H_2}. \qquad (2)$$

The results are summarized in Table 3. For ethane, isobutane, and neopentane, the results of first order with respect to hydrocarbon, and -2.9 to -3.0 order with respect to hydrogen were obtained over the entire measured pressure range (101–20 kPa), irrespective of the catalyst. In the case of *n*-butane the situation was different. As shown in Fig. 3 there were two regions of pressure dependence, one characterized by orders of $n = 1.0$, $m = -3.0$ and one by orders of $n = 0.63$, $m = -1.6$. These values were identical on

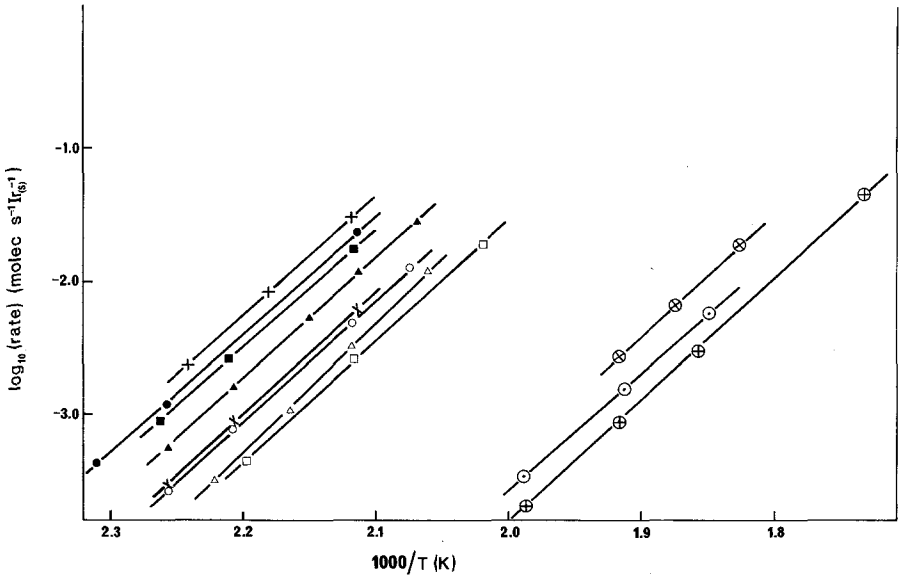

FIG. 1. Arrhenius plots for reactions on supported iridium catalysts. Hydrogen/hydrocarbon molar ratio, 20/1. Hydrocarbon and catalyst type: *n*-butane: +, A_1; ▲, B_1; ●, B_2; ■, B_3. neohexane: ×, A_1; △, B_1; ○, B_2; □, B_3. ethane: ⊕, B_1; ⊙, B_2; ⊗, B_3.

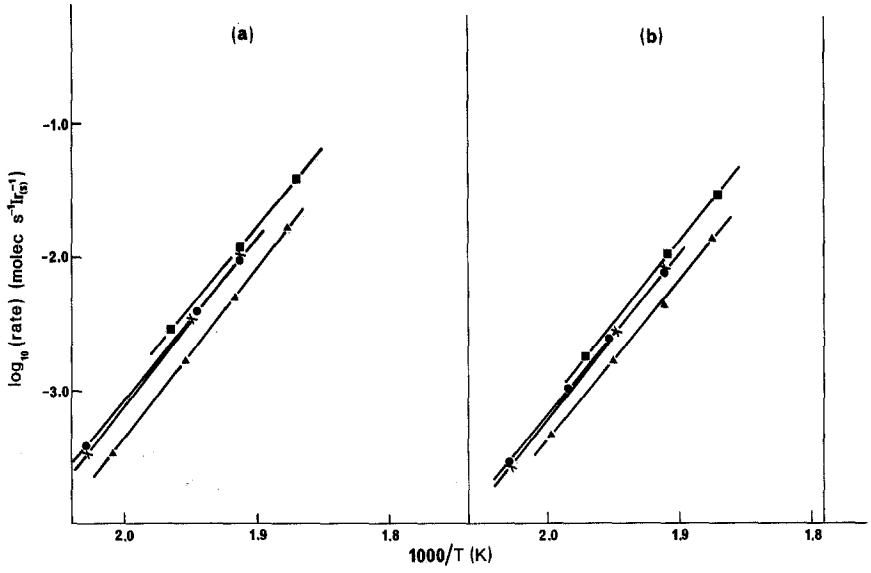

FIG. 2. Arrhenius plots for reactions on supported iridium catalysts. Hydrogen/hydrocarbon molar ratio, 20/1. Hydrocarbon and catalyst type: (a) isobutane: ×, A_1; ▲, B_1; ●, B_2; ■, B_3. (b) neopentane: ×, A_1; ▲, B_1; ●, B_2; ■, B_3.

all catalysts, but the hydrogen pressure where the changeover occurred was a function of the catalyst dispersion. The reaction orders changed at about 40 to 45 kPa on highly dispersed iridium and at about 70 kPa on iridium of low dispersion.

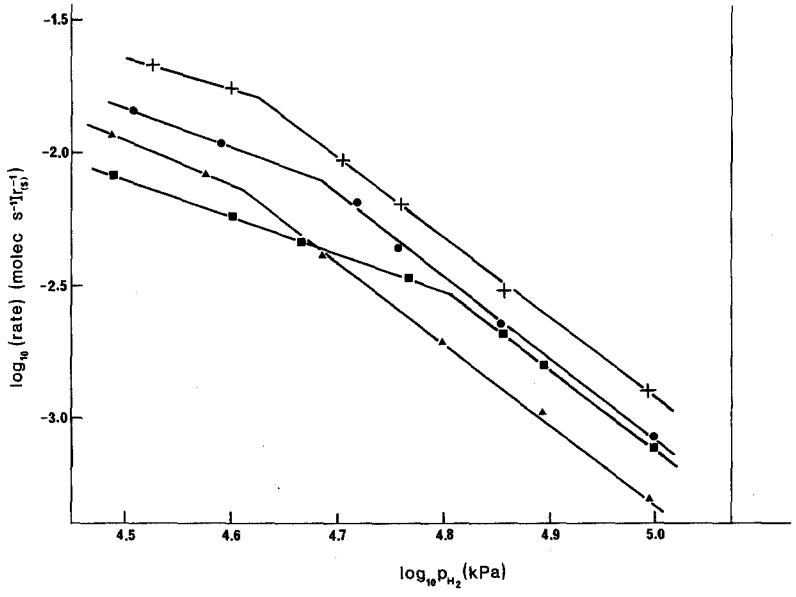

FIG. 3. Variation of reaction rate of *n*-butane with hydrogen pressure over supported iridium catalyst. Reaction temperature 453 K: *n*-butane pressure, 1.3–1.6 kPa. Catalyst: +, A_1; ▲, B_1; ●, B_2; ■, B_3.

TABLE 3

Kinetic Pressure Dependence Exponents

Hydrocarbon	Catalyst	Pressure range (kPa)	Exponents in rate $\propto P^n_{HC} P^m_{H_2}$
Ethane	B_1, B_2, B_3	P_{H_2}, 20–101 P_{HC}, 1.2–10	$n = 1.0$, $m = -2.9$
Isobutane	A_1, B_1, B_2, B_3	P_{H_2} 20–101 P_{HC}, 1.3–12	$n = 1.0$, $m = -2.8$
Neopentane	A_1, B_1, B_2, B_3	P_{H_2}, 20–101 P_{HC}, 1.3–12	$n = 1.0$, $m = -2.9$
n-Butane	A_1, B_1	P_{H_2}, 30–101 P_{HC}, 1.3–12	$n = 1.0$, $m = -3.0$
		P_{H_2}, 18–30 P_{HC}, 1.2–6	$n = 0.6_3$, $m = -1.5$
	B_2	P_{H_2}, 35–101 P_{HC}, 1.3–12	$n = 1.0$, $m = -2.9$
		P_{H_2}, 18–35 P_{HC}, 1.2–6	$n = 0.6_4$, $m = -1.5_5$
	B_3	P_{H_2}, 50–101 P_{HC}, 1.3–12	$n = 1.0$, $m = -2.9$
		P_{H_2}, 18–50 P_{HC}, 1.3–8	$n = 0.6_3$, $m = -1.5_5$

The distribution of initial reaction products was the same in the two pressure dependence exponent regimes.

Product Distributions

The initial product distributions obtained from *n*-butane, isobutane, neopentane, and neohexane on various iridium catalysts are listed in Table 4. Ethane, which yielded only methane, is not included in Table 4. The initial product distributions were, to better than 2% variation, independent of temperature over the reaction-temperature range.

The product distributions at finite conversions of course differ somewhat from the initial distributions. The extent of this difference depends on the reaction conditions and on the reactivity of the primary reaction products compared with the reactant itself. Thus, since neopentane is considerably less reactive than neohexane, secondary reaction of the neopentane product from the primary reaction of neohexane is negligible over the entire range 443 to 495 K. With the other reactant hydrocarbons, secondary reactions occurred to some extent, although as the data in Table 5 make clear by comparison with Table 4, the difference is not large and correction can be easily made with good accuracy, particularly since the low reactivity of ethane compared with the butanes (cf. relevant frequency factors in Table 2) makes secondary reaction of ethane of negligible importance.

The distribution of products obtained from methylcyclopentane is summarized in Table 6.

The reaction of 2,3-dimethylbutane was also studied at the single temperature of

TABLE 4

Distributions of Initial Products

Hydrocarbon	Catalyst	Initial product distribution (mol%)[a]					
		M	E	P	i-B	i-P	neo-P
n-Butane	A_1	13.0	74.0	13.0	—	—	—
	A_2	7.3	85.4	7.3	—	—	—
	B_1	15.3	79.4	15.3	—	—	—
	B_2	20.0	60.0	20.0	—	—	—
	B_3	31.8	36.4	31.8	—	—	—
	A_3	30.4	39.2	30.4	—	—	—
Isobutane	A_1	55.2	23.8	21.0	—	—	—
	B_1	52.4	23.1	24.5	—	—	—
	B_2	54.5	23.3	22.2	—	—	—
	B_3	53.7	18.3	26.4	—	—	—
Neopentane	A_1	60.1	9.5	2.7	27.7	—	
	B_1	58.4	8.4	2.2	31.0	—	
	B_2	58.1	8.7	2.5	30.7	—	
	B_3	56.7	6.6	3.2	24.1	9.4	
	A_3	55.3	5.9	2.5	26.2	10.1	
Neohexane	A_1, A_2, A_3 / B_1, B_2, B_3	50.0	—	—	—	—	50.0

[a] M, Methane; E, ethane; P, propane; i-B, isobutane; i-P, isopentane; neo-P, neopentane. Initial product distributions refer to the reaction temperature range: they are independent of temperature over this range with a variation of not more than about 2%.

495 K, and the product distribution data are summarized in Table 7.

Temperature-Programmed Desorption of Hydrogen

TPD profiles (300–800 K) obtained from hydrogen adsorption at 295 K on iridium catalysts with varying dispersions are shown in Fig. 5. A comparison of curves 1, 2, and 3 indicates a strong particle size dependence of the nature of the TPD profiles. The main desorption peak shifted from 418 to 511 K when the particle size decreased from 7.0 to $\leqslant 1.5$ nm. This shift was accompanied by profile broadening toward the high temperature profile tail. The amounts of hydrogen desorbed after equilibration at 295 K corresponded to about 90 to 95% ot the uptake measured volumetrically.

DISCUSSION

Hydrogenolysis

From the kinetic parameters in Table 2, we are able to distinguish two types of hydrogenolysis reactions on iridium catalysts, involving: (i) bond rupture of the type C_I–C_I, C_I–C_{II}, C_{II}–C_{II}, with an activation energy in the region of 175 kJ mol^{-1}, and (ii) bond rupture of the type C_I–C_{III}, C_I–C_{IV}, C_{II}–C_{IV}, C_{II}–C_{III}, with an activation energy in the region of 235 kJ mol^{-1}.[1]

Bearing in mind the probable error in the activation energy values, it is clear that the activation energy is essentially constant and independent of catalyst type (independent of $\bar{d}_{Ir}$) within each of the

[1] C_I, ..., C_{IV} are defined as primary, ..., quaternary carbon atoms, respectively.

TABLE 5

Distriburions of Products at Finite Conversions

Hydrocarbon	Catalyst and reaction temperature (K)	Product distribution (mol%)[a]					Space velocity (s^{-1})	Conversion Percentage
		M	E	P	i-B	i-P		
n-Butane	A_1 453	13.6	76.5	9.9	—	—	4	7.0
	B_3 453	33.6	37.9	28.7	—	—	4	3.8
Isobutane	A_1 523	57.3	25.6	17.1	—	—	6.5	8.5
	B_3 523	54.2	19.1	26.7	—	—	6.5	10.0
Neopentane	A_1 523	61.4	11.3	2.5	24.8	—	6.5	7.2
	B_3 523	56.8	8.3	4.7	23.2	7.0	6.5	9.1

[a] M, Methane; E, ethane; P, propane; i-P, isopentane.

above groups. We conclude that within each group the hydrogenolysis mechanism is basically the same, but there is a difference in mechanism between the two groups.

A similar pattern is found from the frequency factor (Table 2). Except for ethane which is exceptional and which will be discussed later, the frequency factor for the hydrogenolysis reaction is constant within each group—about 10^{17} molecules s^{-1} $Ir^{-1}_{(s)}$ for group (i) and about 10^{21} molecules s^{-1} $Ir^{-1}_{(s)}$ for group (ii). These kinetic parameters also summarize the relative reactivities of the various bond types, and again setting ethane to one side as an exception, it is clear that hydrogenolysis of group (i) bonds occurs much more readily than of group (ii) bonds.

The data show that with isobutane, *n*-butane, and neohexane, only hydrogenolysis products were observed. With isobutane and neohexane, the mode of reaction (initial product distribution) was independent of catalyst type (independent of $\bar{d}_{Ir}$) and of temperature. On the other hand, with *n*-butane the initial product distribution was significantly dependent on $\bar{d}_{Ir}$. With *n*-butane reaction may occur by rupture of a C_I–C_{II} (terminal) bond to give methane and propane, or by rupture of the C_{II}–C_{II} (central) bond to give ethane. Over catalysts with $\bar{d}_{Ir} \leqslant 1$ to 1.5 nm the reaction was strongly selective toward C_{II}–C_{II} (central) bond rupture, by

TABLE 6

Distribution of Products from Methylcyclopentane

T (K)	C_n products with $n \leqslant 5$ (%)	2-MP/3-MP[a]
419	0	2.10
433	0	2.03
453	4.5[b]	2.10

[a] 2-MP, 2-Methylpentane; 3-MP, 3-methylpentane. Catalyst: B_2 (d_{Ir} = 1.5 nm). Conversion: 1–5 mol%. Space velocity: 13 s^{-1}.

[b] Composition (mol%): CH_4, 35.0; C_2H_6, 18.7; C_3H_8, 9.3; i-C_4H_{10}, 16.8; *n*-C_4H_{10}, 3.3; i-C_5H_{12}, 16.8; *n*-C_5H_{12}, 0.

TABLE 7

Distribution of Products from 2,3-Dimethylbutane[a]

Product	Mole percent
Methane	55.1
Ethane	1.7
Propane	3.7
Isobutane	4.6
Isopentane	34.8

[a] Reaction temperature: 495 K. Catalyst: B_2 (d_{Ir} = 1.5 nm). Conversion: 9.8 mol%. H_2/hydrocarbon ratio, 26/1.

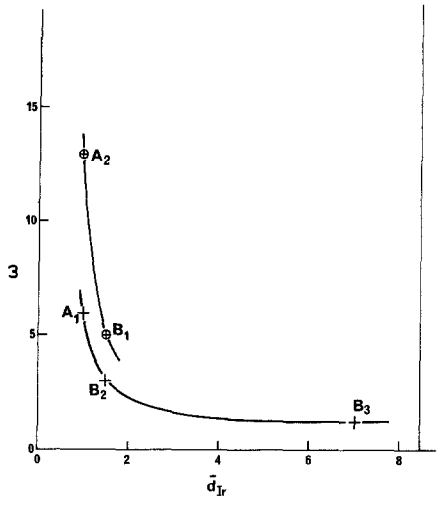

FIG. 4. Variation of ratio: rate of central bond rupture/rate of terminal bond rupture, (ω), in n-butane as a function of average iridium particle size ($\bar{d}_{Ir}$). Reaction temperature, 473 K. Space velocity, 13.4 s^{-1}. Hydrogen/hydrocarbon ratio, 20/1. Points A_2 and B_1 are for Ir/γ-Al_2O_3; A_1, B_2, B_3 are for Ir/SiO_2.

comparison with which reaction over catalysts with $\bar{d}_{Ir}$ of 7 and 20 nm gave more nearly nonselective bond rupture. Figure 4 shows the dependence of the ratio of central bond rupture to terminal bond rupture on $\bar{d}_{Ir}$. This preference for central bond rupture at very low values of $\bar{d}_{Ir}$ is somewhat more pronounced with Ir/γ-Al_2O_3 than with Ir/SiO_2.

Since these product distributions were temperature invariant one must conclude that central bond rupture and terminal bond rupture occur with equal activation energies, and the changing selectivity with $\bar{d}_{Ir}$ occurs solely by a difference in the frequency factor for the two processes.

Extensive central bond rupture in n-butane hydrogenolysis has been reported by Plunkett and Clarke (*4*) for iridium–gold film catalysts of relatively high gold content ($\geqslant$86 mol% Au). In this respect, these alloy catalysts of very large metallic particle size resemble pure iridium catalysts of very small metallic particle size.

Isomerization

In our results, significant isomerization product was observed from the reaction of

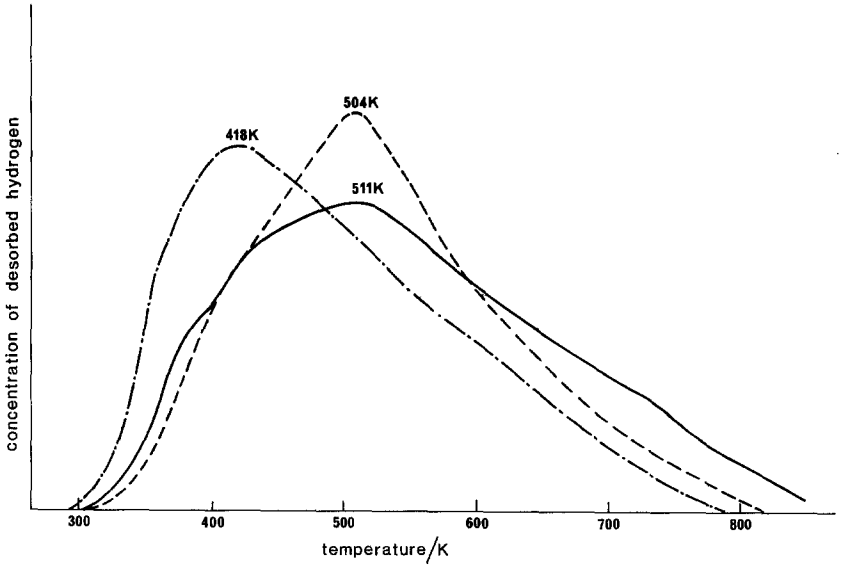

FIG. 5. Temperature desorption profiles for hydrogen from reduced supported iridium catalysts. Hydrogen adsorption at 293 K and samples then equilibrated in sweep gas at 293 K. Heating rate, 25 K min^{-1}. Starting temperature, 300 K. Catalysts: ——, B_1; – – –, B_2; —·—·—·, B_3.

neopentane over catalysts with $\bar{d}_{Ir}$ of 7 and 20 nm, but none with catalyst having $d_{Ir} \leqslant 1$ and 1.5 nm. In comparison with this, Boudart (*7*) reported that an iridium/silica catalyst with $\bar{d}_{Ir}$ of 1.5 nm showed isomerization activity for neopentane. Since the reaction conditions used by Boudart were fairly similar to those used in the present work, we consider this difference with the present results to be real, and we suggest it may have been due to the presence in Boudart's catalyst of a proportion of relatively large iridium particles which were active for isomerization. This suggestion is made probable by noting that Boudart's catalyst had the relatively high metal loading of 10 wt%, and the value of $\bar{d}_{Ir}$ had been estimated from adsorption data which are dominated by the small particle end of the size distribution range. Furthermore, an electron microscopic study of our well-dispersed iridium catalysts ($d_{Ir} \leqslant 1$ and 1.5 nm) showed a relatively narrow size distribution range, with the total absence of large particles, and an upper limit to the particle size distribution of about 2 nm.

The product distributions from isobutane also suggest that a portion of this reaction may have occurred via isomerization to *n*-butane followed by hydrogenolysis. This conclusion is inevitable if it is assumed that only one carbon–carbon bond is ruptured in the initial reaction of any hydrocarbon and this assumption certainly is substantiated by the behavior of *n*-butane. In the case of isobutane, the generation of substantial and comparable amounts of ethane and propane can then be accounted for if part of the isobutane has undergone preliminary isomerization to *n*-butane. Although this is an inferential conclusion, it is supported by the observation of Karpinski and Clarke (*5*) that some *n*-butane was formed from isobutane over iridium film catalysts at 529 to 614 K (hydrogen/hydrocarbon reactant ratio, 10/1).

Temperature-Programmed Desorption of Hydrogen

The change in the shape of the TPD profiles with varying $\bar{d}_{Ir}$ (cf. Fig. 5) means that at small values of $\bar{d}_{Ir}$ there is an increased proportion of higher energy binding states for hydrogen. This trend is similar to that already reported with platinum (*11*), but it is more pronounced with iridium.

This implies that the concentration of hydrogen chemisorbed on the iridium surface at reaction temperature will be a function of $\bar{d}_{Ir}$. This is shown in Fig. 6, where we have plotted, as a function of temperature (T) for various $\bar{d}_{Ir}$, values for the ratio n_T/n_{295}, where n is the quantity of hydrogen desorbed in the TPD profile at temperatures above the specified temperature (TK or 295 K). The data in Fig. 6 cannot be used to make quantitative comparisons of hydrogen coverages under actual reaction conditions because the gas-phase hydrogen pressures are considerably different in a reaction mixture and under TPD conditions; furthermore, under reaction conditions there will be competition for adsorption sites by other reactant molecules.

Nevertheless, the data summarized in Fig. 6 clearly demonstrate a trend of higher hydrogen concentration at lower $\bar{d}_{Ir}$.

Kinetic Pressure Dependence

Literature data for kinetic pressure dependence exponents on iridium for the molecules examined in the present study are not available except for ethane; Sinfelt (*6*) reported exponents of $n = 0.7$ and $m = -1.5$ (for ethane and hydrogen, respectively). These values are considerably different from those found in the present work ($n = 1.0$ and $m = -2.9$; cf. Table 3). However, Sinfelt's data were obtained at pressures below the lower pressure limits used in our study, and it is possible that, as the pressures are reduced, the reaction

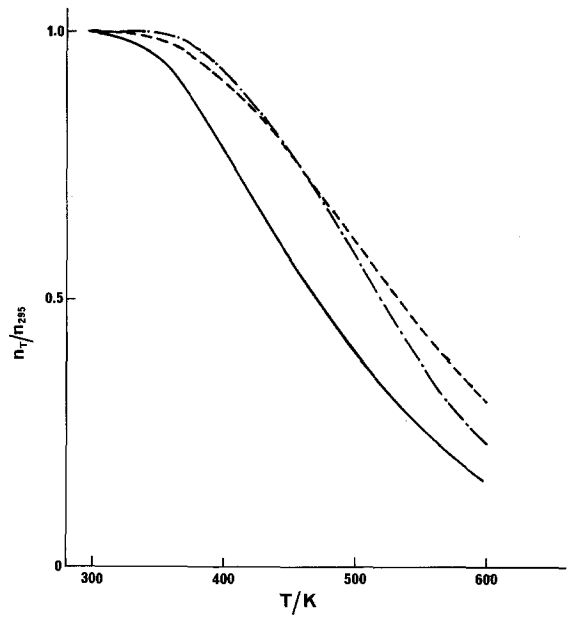

FIG. 6. Dependence of n_T/n_{295} on temperature T(K). n_T, quantity of hydrogen desorbed in TPD profile at temperatures above T(K); n_{295}, quantity of hydrogen desorbed in TPD profile at temperatures above 295 K. Primary data from Fig. 5. Curve ——, $\bar{d}_{Ir}$ = 7.0 nm (catalyst B_3); curve —·—·—·, $\bar{d}_{Ir}$ = 1.5 nm (catalyst B_2); curve — — —, $\bar{d}_{Ir}$ = 1.5 nm (catalyst B_1).

orders for ethane change in a manner similar to that observed with *n*-butane (cf. Table 3).

Provided the hydrogen pressure is high enough, it is evident from Table 3 that the kinetic orders in hydrocarbon and hydrogen are virtually invariant, irrespective of hydrocarbon type or of $\bar{d}_{Ir}$; i.e., $n = 1.0$, $m \approx -3$. This suggests that, if adsorption to form the reaction intermediate is written as

$$C_xH_{2x+2(g)} \rightleftharpoons [C_xH_{2x+2-y}]_{(s)} + yH_{(s)}, \quad (3)$$

with

$$H_{(s)} \rightleftharpoons \tfrac{1}{2}H_{2(g)}, \quad (4)$$

the extent of dehydrogenation to form $[C_xH_{2x+2-y}]_{(s)}$ is about the same for all hydrocarbons.

Assuming that carbon–carbon bond rupture in $[C_xH_{2x+2-y}]_{(s)}$ is rate controlling, it is possible to construct a scheme which allows the value of y in $[C_xH_{x+2-y}]_{(s)}$ to be expressed in terms of the pressure dependence exponents n and m, in the manner first outlined by Cimino *et al.* (*14*).

However, this approach cannot do more than give a very rough indication of the extent of dehydrogenation of the adsorbed reaction intermediate because the treatment contains some parameters which are unlikely to be known *a priori*—for instance, the nature of the hydrogen adsorption isotherm under reaction conditions (high or low hydrogen coverage) and whether in the rate-controlling step the adsorbed hydrocarbon residue is attacked by $H_{2(g)}$ or $H_{(s)}$. In the present case, this treatment indicates that the adsorbed reaction intermediate is extensively dehydrogenated, with a value of y in $[C_xH_{2x+2-y}]_{(s)}$ in the range 3 to 6 depending on the assumptions used in the model.

Despite this uncertainty this general method of approach does allow the abnormally low frequency factor for the

ethane reaction (cf. Table 2) to be rationalized relative to the frequency factors for *n*-butane and neohexane which, together with ethane, all have about the same activation energy.

Consider the reaction

$$C_xH_{2x+2(g)} \rightleftharpoons [C_xH_{2x+2-y}]_{(g)} + y/2H_{2(g)} \quad (5)$$

It is probable that, in forming the adsorbed reaction intermediate, we must have $y > 2$. This is suggested by the values of y indicated above and is supported both by previous estimates (*6*), and by arguments based upon the ease or rupture of various types of carbon–carbon bonds (*vide infra*). We shall thus compare equilibrium constants for reaction (5) at 500 K (K_{500}) for the case $y = 4$, and the alternative values $x = 2$ (ethane to ethyne) and $x = 4$ (*n*-butane to but-2-yne).

$$\left.\begin{matrix} x = 2 \\ y = 4 \end{matrix}\right\} \quad K_{500} = 7.6 \times 10^{-21} \text{ atm}^2.$$

$$\left.\begin{matrix} x = 4 \\ y = 4 \end{matrix}\right\} \quad K_{500} = 9.3 \times 10^{-17} \text{ atm}^2.$$

From this it follows that if the free energy of adsorption is about the same for C_2H_2(g) and $C_4H_{6(g)}$, the concentration of adsorbed intermediate from ethane would be considerably less than from *n*-butane, as required to account for the difference in frequency factors.

The reaction of *n*-butane shows two regions with different pressure dependence exponents, depending on the hydrogen pressure. This is the same sort of behavior as has been previously reported for the reaction of neopentane over platinum (*10*, *13*), and we attribute it to an increased relative coverage by adsorbed hydrocarbon, and a corresponding decreased hydrogen coverage at lower hydrogen pressures. The change in the transition hydrogen pressure with $\bar{d}_{Ir}$ is consistent with the increased hydrogen coverage at smaller $\bar{d}_{Ir}$ indicated by the TPD results. Since the product distributions are the same in the two pressure dependence exponents regimes, we conclude that the nature of the adsorbed hydrocarbon reaction intermediate is the same in both cases.

Reaction Modes

It is convenient first to discuss the comparative behavior of the various hydrocarbons over iridium catalysts in terms of two archetypal reactions. Ethane is the archetype for hydrogenolysis with a relatively low activation energy in the region of 175 kJ mol^{-1}. Since this involves carbon–carbon bond rupture in a skeletal unit consisting of only a pair of adjacent carbon atoms, we shall refer to it as hydrogenolysis in a C_2-unit mode.

Bearing in mind the kinetic similarity of neopentane and isobutane for hydrogenolysis over iridium, we shall refer to the archetype which is characterized by the relatively high activation energy in the region of 235 kJ mol^{-1}, as hydrogenolysis in an iso-unit mode.

Previous work has also reported that the activation energy for the reaction of ethane over dispersed iridium is some 40 to 50 kJ mol^{-1} lower than that for neopentane, although the absolute magnitudes are somewhat lower than those found in the present work. Thus, Sinfelt (*6*) has reported an activation energy of 152 kJ mol^{-1} for ethane, while Boudart (*7*) cites a value of 195 kJ mol^{-1} for neopentane. Nevertheless, the mid-temperature range turnover numbers are in fairly good agreement: at 523 K Sinfelt (*6*) gives a turnover number for ethane of 3.3×10^{-2} molecules s^{-1} Ir$^{-1}_{(s)}$ compared with our value of around 10×10^{-2} molecules s^{-1} Ir$^{-1}_{(s)}$, while for neopentane at 523 K Boudart (*7*) gives a turnover number of 2.6×10^{-2} molecules s^{-1} Ir$^{-1}_{(s)}$ compared with our value of around 2×10^{-2} molecules s^{-1} Ir$^{-1}_{(s)}$. (These comparisons have been made after

extrapolating our data to the pressure conditions used by the other workers).

On this basis then, *n*-butane reacts via the C_2-unit mode. Neohexane, which is of a structure such that hydrogenolysis could, in principle, occur by C_2-unit or iso-unit mode, in fact reacts exclusively via a C_2-unit mode with carbon–carbon bond rupture occurring only in the ethyl group. This is exactly consistent with the expectation that the lower activation energy pathway will be selected if a choice is available.

In this respect, the behavior of iridium is in marked contrast to that of platinum. On platinum, reaction via the C_2-unit mode is relatively difficult and reaction by the iso-unit mode is relatively facile: neohexane for instance, reacts mainly to give ethane and isobutane, while the activation energy for the reaction of ethane is much greater than that for neopentane (*3*).

As noted above on iridium the activation energy for the reaction of isobutane is similar to that of neopentane, even though in terms of the skeletal structure of isobutane, one might have expected the more facile C_2-unit reaction mode to have been available: chemisorption at the tertiary carbon atom of isobutane is possible, but the corresponding process cannot occur at the quaternary carbon atom in neopentane.

We are thus forced to the conclusion that reaction via the C_2-unit mode cannot occur if one of the constituent carbon atoms is tertiary. This is exactly confirmed by the reaction pattern of methylcylcopentane (Table 6) for which hydrogenolysis occurs in a manner that totally excludes the tertiary carbon atom. Carbon–carbon bond rupture is entirely confined to the ring bonds 2–3 and 3–4, where the carbon atoms are all secondary, and here the reactions occur with equal statistical probability, since the product ratio 2-methylpentane/3-methylpentane is very close to 2.

This behavior of iridium with methylcyclopentane is markedly different from that of platinum (*3*). Over highly dispersed platinum, methylcyclopentane undergoes nonselective ring opening; that is, *n*-hexane, 2-methylpentane, and 3-methylpentane are produced in the ratios 2:2:1. On platinum, ring opening of the type found over highly dispersed iridium is only found at very low dispersions.

The behavior of 2,3-dimethylbutane confirms the conclusion that C_2-mode hydrogenolysis is very difficult if one of the carbon atoms is tertiary. In this molecule, the central bond lies between two tertiary carbon atoms, and the data in Table 7 show that essentially no rupture of this bond occurs.

We may thus summarize the situation as follows. Provided the bond in question is of the type C_I–C_I, C_I–C_{II}, C_{II}–C_{II}, reaction occurs via a C_2-unit mode with a lower activation energy in the region of 175 kJ mol^{-1}. Bonds of the type C_I–C_{IV}, C_I–C_{III}, C_{II}–C_{III} react via an iso-unit mode with a higher activation energy in the region of 235 kJ mol^{-1}.

The failure of bonds which contain a tertiary carbon atom to react via a C_2-unit mode implies that, for this mode to operate, each of the constituent carbon atoms must be able to lose at least two hydrogen atoms in the chemisorption process.

In the reactions on iridium with the various hydrocarbons which proceed in the C_2-unit or the iso-unit modes (Table 2), the activation energy is effectively constant over a wide range of $\bar{d}_{Ir}$, from $\leqslant 1$ to 20 nm. We thus conclude that for each of these reaction modes, the basic reaction mechanism does not change as $\bar{d}_{Ir}$ changes, and we therefore infer that for each of these reaction modes the nature of the reaction site does not change as $\bar{d}_{Ir}$ changes.

It follows therefore that for neither of these modes can the reaction site be of a type such that the site density depends on $\bar{d}_{Ir}$. The simplest assumption is to assume that all surface iridium atoms are

equally effective, irrespective of surface geometry. This need not necessarily imply that a reactive site is to be identified with a single iridium atom, merely that if a reactive site consists of a group of surface iridium atoms, then the group is of a structure such that its change of occurrence is independent of $\bar{d}_{Ir}$.

The present results do not allow a more definite assessment of the nature of the reactive sites. Further insight may be possible via a surface ensemble approach using group VIII/group IB alloy catalysts, and experiments of this sort are currently under way in this laboratory.

The insensitivity of the neopentane reaction (iso-unit mode) to $\bar{d}_{Ir}$ is in marked contrast to the behavior of this hydrocarbon over platinum catalysts, where the reaction is strongly dependent on $\bar{d}_{Pt}$ (*10*). These data have led to the conclusion that there are two alternative pathways which are differentiated by the number of surface platinum atoms involved in the reaction sites. Iridium behaves quite differently in that there is no evidence for more than a single process.

The activation energy for the reaction of ethane (C_2-unit mode) is independent of $\bar{d}_{Pt}$ (*3*, *12*, *13*) and, although the frequency factor for this reaction shows a small variation with $\bar{d}_{Pt}$, one may conclude that with ethane (unlike neopentane) the reaction behaves rather similarly toward metallic particle size with both iridium and platinum, and there is no evidence for more than a single process over either metal.

REFERENCES

1. Sinfelt, J. H., U.S. Patent 3,953,368.
2. Rasser, J. C., "Platinum–Iridium Reforming Catalysts." Delft Univ. Press, Delft, 1977.
3. Anderson, J. R., *in* "Advances in Catalysis" (W. G. Frankenburg, V. I. Komarewsky, and E. K. Rideal, Eds.), Vol. 23, p. 1. Academic Press, New York, 1973.
4. Plunkett, T. J., and Clarke, J. K. A., *J. Catal.* **35**, 330 (1974).
5. Karpinski, Z., and Clarke, J. K. A., *J. Chem. Soc. Faraday Trans. I* **71**, 2310 (1975).
6. Sinfelt, J. H., *Catal. Rev.* **3**, 175 (1969).
7. Boudart, M., and Ptak, L. D., J. *Catal.* **16**, 90 (1970).
8. Anderson, J. R., and Avery, N. R., *J. Catal.* **5**, 446 (1966).
9. Anderson, J. R., Mainwaring, D. E., Elmes, P. S., and Howe, R. F., *J. Catal.* **50**, 508 (1977).
10. Foger, K., and Anderson, J. R., *J. Catal.*, **54**, 318 (1978).
11. Anderson, J. R., Foger, K., and Breaksphere, R. J., *J. Catal.*, **57**, 458 (1979).
12. Sinfelt, J. H., Taylor, W. F., and Yates, D. J. C., *J. Phys. Chem.* **69**, 95 (1965).
13. Leclercq, G., Leclercq, L., and Maurel, R., *J. Catal.* **44**, 68 (1976).
14. Cimino, A., Boudart, M., and Taylor, H. S., *J. Phys. Chem.* **58**, 296 (1954).